Applied Catalysis B: Environmental 88 (2009) 299–304

Contents lists available at ScienceDirect

Applied Catalysis B: Environmental

journal homepage: www.elsevier.com/locate/apcatb

Screening of Fe–BEA catalysts for wet hydrogen peroxide oxidation of crude olive mill wastewater under mild conditions

Wahiba Najjar [a,*], Samia Azabou [b], Sami Sayadi [b], Abdelhamid Ghorbel [a]

[a] Laboratoire de Chimie des Matériaux et Catalyse, Faculté des sciences de Tunis, Campus Universitaire, Tunis 2092, Tunisia
[b] Laboratoire des Bioprocédés, Pôle d'Excellence Régional, Centre de Biotechnologie de Sfax, BP « 1177 », 3018 Sfax, Tunisia

ARTICLE INFO

Article history:
Received 16 July 2008
Received in revised form 31 October 2008
Accepted 9 November 2008
Available online 25 November 2008

Keywords:
BEA zeolite
Catalytic wet hydrogen peroxide oxidation
Iron
Olive mill wastewater

ABSTRACT

A series of Fe–BEA catalysts, differing in the amount of iron have been characterized by XRD, BET surface area, UV–vis spectroscopy and chemical analysis. The zeolite samples have been tested as heterogeneous catalysts for the wet hydrogen peroxide oxidation of crude olive mill wastewaters (OMW) under very mild conditions (at 28 °C and atmospheric pressure). All experiments were performed on a laboratory scale set-up.

BSE-1/3 catalyst with a moderate Fe content (Fe/Al = 1.19) showed the best results in terms of catalytic activity and loss of active species into the aqueous solutions. The stability of Fe species has been shown to be strongly dependent on the Fe environment into the zeolite framework.

Over the selected catalyst, application of catalytic procedure on diluted OMW solution permitted high removal efficiencies of pollutants. The process produces a removal capacity of 28% of total organic carbon (TOC), 40% of total phenols, 30% of chemical oxygen demand (COD) and 59% of colour, just after 12 h. 5-Day biochemical oxygen demand (BOD_5), and toxicity towards the bioluminescent bacteria *Vibrio fischeri* were selected to follow the performance of this process in terms of reducing the ecotoxicity of OMW. Results showed an increase in the biodegradability of the treated sample and a decrease of the microtoxicity from 100% to 70% load towards *V. fischeri*.

Occurrence of small catalyst deactivation by carbonaceous during the oxidation reaction was observed through scanning electron microscopy (SEM) and elemental analysis.

1. Introduction

The olive oil extraction industries in the Mediterranean countries generate each year an increasing volume of olive mill wastewater (OMW) with a great pollutant influence. Tunisia is one of the largest olive oil producers in the world with an average annual production of 450,000 tons. This results in a byproduct of 6,000,000 m^3 OMW. This liquid residue is a serious environmental problem due to its high organic fraction including sugars, tannins, acids, pectins, lipids and especially phenols and polyphenols which are known to be biorecalcitrant [1,2]. OMW is characterized by a high chemical oxygen demand (COD) imposing problems at the time of proper management and disposal. COD of this type of effluents ranges between 25 and 300 g O_2 L^{-1} in the worst of the cases [3]. The high risk to produce irreversible environmental problems caused by this type of residue makes necessary the use of appropriate technologies to reduce toxic compounds, especially the phenolic content.

In recent times, most of the studies about OMW treatments are focused on aerobic [4] or anaerobic digestion [5,6]. However problems concerning the high toxicity and the biodegradability of the effluents have been encountered during these anaerobic treatments [7], and the experimental results are not satisfactory: they must be conducted on a highly dilute substrate once the aromatic and phenolic compounds are toxic for methanogenic bacteria [8,9]. Among the variety of wastewater treatment technologies, advanced oxidation processes (AOPs) have emerged as interesting alternative for the destruction of organic pollutants in industrial wastewater. These processes basically involve the generation of reactive hydroxyl radicals ($OH^{\bullet}$) with high oxidation potential, which are able to mineralize these refractory compounds [10]. Fenton's reagent as oxidation system based on the reaction of H_2O_2 with Fe(II)/Fe(III) ions has been used as a powerful source of oxidative radicals [11,12].

The use of the Fenton's reagent as homogeneous catalyst implies several drawbacks. A limited range of pH (2.5–3.5) has to be used so that the reaction takes place. In a second term, recovery of iron ions from the solution through additional separation steps is needed in homogeneous catalytic systems to comply with environmental regulations. In this sense, a challenging issue is the

* Corresponding author. Tel.: +216 23265760; fax: +216 71885008.
E-mail address: wahiban@yahoo.fr (W. Najjar).

0926-3373/$ – see front matter © 2008 Elsevier B.V. All rights reserved.
doi:10.1016/j.apcatb.2008.11.023

immobilization of iron species over different supports as catalyst for Fenton processes which would also enable its application under non-controlled pH conditions. The use of heterogeneous catalysts could be an alternative method of these problems. Recently, a great number of materials containing iron and copper as precursors supported/intercalated on/in oxides, clays and polymers as active catalysts for Fenton-type reactions have been proposed to remove organic compounds [13–19]. These catalysts exhibit the advantages of heterogeneously catalyzed process and got relatively higher oxidation efficiency as well as a lower sensitivity to pH. However, most of them could not be used due to its lack of stability in aqueous media. A leaching of the active elements or/and the support was often observed [20].

A few studies dealing with the use of zeolites containing copper or iron as catalytic active sites for phenolic compound oxidation were also recently reported [20–27,13,28–31]. The metal bearing zeolites were prepared using classical procedures consisting of generating dispersed Cu^{2+} or Fe^{3+}species anchored to the zeolite framework by ionic exchange of the protonated zeolite with various Cu^{2+}or Fe^{3+}salts. In such systems, however, severe metal leaching was observed, leading to side reactions catalyzed in homogeneous phase [20]. To our knowledge, now results have been reported in the literature concerning the oxidation of OMW over Fe–zeolite catalysts.

The main purpose of this work is to assess the catalytic performance of a wide series of iron bearing beta zeolites systems taking into account their activity and stability in catalytic wet hydrogen peroxide oxidation (CWHO) of OMW.

Because of its unique properties, beta zeolite has been extensively used as a catalyst support for active iron metal dedicated to wet hydrogen peroxide oxidation (WHO) of organic pollutants. Beta (BEA framework class) is a well-known class of zeolites the use of which is considerably expanding due to the interesting properties in the alkylation of aromatics [32]. The BEA ring channels have significantly larger internal accessibility than the MFI ring framework [33]. On the other hand, BEA zeolites show analogies with MFI zeolites in terms of the other framework characteristics (three-dimensional pore network, topology) and therefore are suitable candidates to develop Fe/zeolite materials which may be used for catalytic wet hydrogen peroxide oxidation of diluted OMW.

Iron–BEA catalysts have been prepared by the solid iron exchanged method to generate Fe–BEA catalysts involving iron species more strongly bonded to the zeolite framework, possibly less ready subject to extensive leaching during catalytic treatments. A detailed investigation by XRD, BET surface area, UV–vis spectroscopy and chemical analysis has been carried out. The catalytic performance has been determined in terms of phenol, TOC, COD, BOD_5 and colour conversions. The effect of treatment on OMW acute ecotoxicity was investigated.

In addition, the stability of the catalyst was also studied in terms of metal leaching. The environmental impact of the process was evaluated.

Furthermore, the deactivation by carbon formation being a very important aspect of the catalytic chemistry of these materials during the oxidation reaction was observed through scanning electron microscopy (SEM) and elemental analysis.

2. Experimental

2.1. Starting materials

The support used is a beta zeolite (BEA framework class) with an Si/Al ratio of 50. The BEA framework is characterized by 12 member ring channels (the 12 member ring along the [1 0 0] direction has openings of 0.66 nm × 0.67 nm, and along the [0 0 1] direction openings of 0.56 nm × 0.56 nm) having significantly larger internal accessibility that the 10 member ring of the MFI framework (the 10 member ring along the [1 0 0] direction has openings of 0.51 nm × 0.55 nm, and along the [0 1 0] direction openings of 0.53 nm × 0.56 nm) [33].

2.2. Catalyst synthesis

The catalysts were prepared by the solid ion exchange method. Typically, 2 g of BEA zeolite was intimately mixed with the desired percentage of Fe [$Fe(NO_3)_3{\cdot}9H_2O$] in an agate mortar for 15 min, followed by heating at 523 K for 12 h. The resulting samples were cooled to the ambient temperature, washed with distilled water, filtered, oven dried at 333 K, and calcined at the desired temperature. The calcined catalysts are referred to (BSE-1/12, BSE-1/6, BSE-1/3 and BSE-2/3).

2.3. Characterization methods

XRD analyses were performed on oriented samples prepared by spreading of the sample suspension on a glass slide, followed by drying at room temperature. The XRD patterns were obtained with a PW 1130/00/60 Philips diffractometer using CuK_α radiation (λ = 1.5405 Å). Chemical analysis was carried out on a Perkin Elmer 3100 spectrometer after dissolution of the sample with several acids (HF, $HClO_4$, HCl) for 24 h, and HNO_3 in a second time.

BET surface areas and porosities were determined with an ASAP 2000 apparatus coupled with an A.S.I. computer. The samples were previously outgassed at 200 °C in an automatic mode.

UV–vis diffuse reflectance spectra of the catalyst was obtained for the dry pressed disk samples using UV–vis spectrophotometer Perkin Elmer Lambda 45 between 200 and 900 nm range. Absorption spectrum was referenced to BaSO4. The main textural characteristics of the catalyst are gathered in Table 1.

Catalyst morphology was examined by SEM on a PHILIPS XL 30 microscope operating at acceleration voltages = 15–25 kV and magnification values up to 1400×. Samples were dusted on a double-sided sticky tape and mounted on microscope slides. Energy dispersion X-ray (EDX) spectra for the fresh and used catalyst samples were recorded using an instrument consisting of a scanning electron microscope and X-ray microanalyzer EDAX 9100/60 (PHILIPS).

2.4. Olive mill wastewater

The original OMW used for experiments was obtained from an olive oil mill in Sfax, home of the olive growing and processing sector, in the southern part of Tunisia. The traditional discontinuous method has been used for the oil extraction. The fresh OMW was firstly centrifugated (6000 trs/min) during 20 min, in order to remove large grease drops and solid particules, which could affect the catalytic reaction behaviour. OMW characteristics was gathered in Table 2.

Table 1
Characterization of Fe–BEA catalysts.

Sample	Crystallinity (%)	S_{BET} (m^2/g)	$V_{microporous}$ (cm^3/g)	Fe/Al
BEA	100	520	0.182	–
BSE-1/12	98	493	0.163	0.27
BSE-1/6	97	469	0.162	0.52
BSE-1/3	98	457	0.155	1.19
BSE-2/3	98	460	0.149	1.87

Table 2
Physico-chemical characteristics of crude OMW.

Characteristics	Mean value
PH	5.2
Salinity (g/L)	18.3
Total solids (g/L)	61.9
TOC (g/L)	26.0
COD (g/L)	64.4
BOD_5 (g/L)	13.7
COD/BOD_5	4.7
Total phenols (g/L)	6.4

2.5. Olive mill wastewater oxidation

Crude OMW oxidation was carried out in a 250-mL Pyrex reactor equipped with a magnetic stirrer. The solid catalyst was introduced into 100 mL of diluted crude OMW under continuous stirring. The desired quantity was added, indicating the start of the reaction. The initial H_2O_2 concentration is equal to 2×10^{-2} M. Blank experiments using no catalyst, but in the presence of H_2O_2 were also performed.

Samples of the reaction medium were withdrawn at regular intervals, and immediately analyzed. The total organic carbon in the supernatant was measured for establishing the degree of conversion. Phenolic compounds were analyzed after separation of the catalyst by a 0.45-μm Millipore filter and ethyl acetate extraction, using HPLC.

2.6. Extraction and analytical methods

The extraction process was applied three successive times to 100 mL of the sample using an equal volume of ethyl acetate to extract the aqueous phase, thus obtaining a representative residue of the phenol content in the OMW. This residue was redissolved in 1 mL of ethyl acetate. The phenol content was identified and quantified using HPLC.

HPLC analysis used for monomeric phenols was performed on a Shimadzu apparatus composed of a pump (LC-10ATvp) and a UV detector (SPD-10Avp). The column used to analyze phenols was C-18 (4.6 mm × 250 mm) Shim-pack VP-ODS. Eluates were detected at 280 nm. The temperature was maintained at 40 °C. The mobile phase used was 0.1% phosphoric acid (Prolabo, France) in water versus 70% acetonitrile (Dharmadrug GmbH, Germany) in water for a total running time of 50 min. The flow rate was 0.6 mL/min, and the injection volume was 50 μL.

TOC analyser (TOC-5050A, Shimadzu) was employed to measure TOC in the sample solution.

The microtoxicity test consists of the inhibition of the bioluminescence of *Vibrio fischeri* LCK480 using the (Dr. Lange GmbH, Düsseldorf, Germany) LUMIStox system and according to ISO 11348-2 [34]. Percentage inhibition of the bioluminescence was achieved by mixing 0.5 mL of OMW and 0.5 mL luminescent bacterial suspension. After a 15-min exposure at 15 °C, the decrease in light emission was measured. The toxicity of the sample is expressed as the percent of the inhibition of bioluminescence ($\%I_B$) relative to a non-contaminated reference. A positive control (7.5% NaCl) was included for each test.

COD was determined according to Knechtel standard method in acidic media and in the presence of potassium bichromate solution [35]. The analysis was realized in a test tube containing 2.5 mL of sample, 1.5 mL of aqueous potassium bichromate solution ($K_2Cr_2O_7$, $HgSO_4$ and H_2SO_4) and 3.5 mL of H_2SO_4 containing $AgSO_4$.

BOD_5 was determined by the manometric method with a respirometer (BSB-Controller Model 620 T (WTW)). Total phenolic concentrations were quantified by means of Folin–Ciocalteau colorimetric method using gallic acid as standard [36]. The absorbance was determined at $\lambda = 725$ nm. The process was described elsewhere [37].

3. Results and discussion

Fe-containing zeolitic materials with different Fe contents have been synthesized as described in Section 2 and tested on the CWHO of diluted OMW (TOC = 1300 mg/L). The catalytic performance of the different zeolite matrix has been evaluated in terms of phenolic OMW compound and TOC removals with a minimum leaching of iron species into the solution.

It should be noted that pH was not adjusted at the beginning of experiments and OMW samples were directly used at their natural pH (5.2) since it was found to be in the optimum range close to 5 of catalytic oxidation reaction.

3.1. Preliminary experiments

A first oxidation reaction was performed on diluted OMW solution (TOC = 1300 mg/L, COD = 3.2 g/L, pH 5.2) at 28 °C and atmospheric pressure, in the presence of H_2O_2 as the oxidant agent but without catalyst. Fig. 1 shows a low OMW phenolic compound conversion (10%) and a negligible TOC removal (4%) after 24 h reactions. An additional catalytic reaction was carried out under the same experimental conditions in the presence of BSE-1/3 catalyst and H_2O_2. It can be seen from Fig. 1 that the presence of both catalyst and H_2O_2 permitted high removal efficiencies of pollutants. After 24 h of reaction, 52% and 33% conversion were obtained respectively for OMW phenolic pollutants and TOC. These oxidation processes in the liquid phase are promoted by the generation of different radical species such as organic hydroperoxyl ($ROO^{\bullet}$), hydroxyl ($OH^{\bullet}$) and hydroperoxyl ($HO_2^{\bullet}$), whose formation rate is significantly enhanced in the presence of metallic species [38,39].

3.2. Catalyst screening

High H_2O_2 decomposition and decrease in TOC values are necessary, but not sufficient, for a catalyst to be considered as efficient. The presence of metallic cations in the solution, which will cause additional pollution, has to be avoided.

Table 3 presents the specific initial rate of OMW phenolic compound oxidation, the TOC abatement and the iron leaching after 24 h of OMW degradation using the different zeolite matrix. At the end of experiments, the pH values were in the range of 4.6–4.8. Catalytic oxidation reaction of phenolic solution is usually accompanied by carboxylic acids formation as reaction intermediates which result in pH decrease. The weak decrease in pH

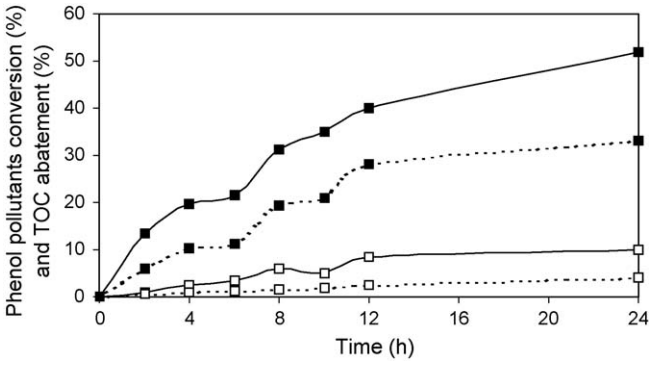

Fig. 1. Phenol pollutants conversion (—) and TOC abatement (···) during the OMW oxidation by: H_2O_2 (□) and H_2O_2/BSE-1/3 (■). Experimental conditions: TOC_{OMW} = 1300 mg/L, pH 5.2, T = 298 K, $[H_2O_2] = 2 \times 10^{-2}$ M, $m_{BSE\text{-}1/3}$ = 0.5 g/L.

Table 3
Catalytic properties of different Fe–BEA catalysts for CWHO of OMW after 24 h and specific initial rate of OMW phenolic compound oxidation.

Sample	V_0 ($\times 10^3$ mol L^{-1} h^{-1} g^{-1})	TOC removal (%)	Fe leaching (ppm)
No catalyst	0.5	4	–
BSE-1/12	3.1	20	3.2
BSE-1/6	4.2	30	3.4
BSE-1/3	6.3	33	3.8
BSE-2/3	5.7	28	4.8

values after the CWHO of OMW in our study could be attributed to the buffer character of OMW due to the presence of bicarbonate species.

Table 3 shows that the specific initial oxidation rate and the TOC removal over different Fe–zeolites increase with respect to the increase of catalyst iron content. Unfortunately, a decrease of the specific initial oxidation rate and the TOC abatement for BSE-2/3 matrix was found. The stability of Fe–zeolite catalysts in terms of iron leaching depends on their iron contents. The leaching is at the same level for BSE-1/12, BSE-1/6 and BSE-1/3 catalysts, but increase for BSE-2/3 matrix, which suggests the coexistence of different Fe environments in the synthesized Fe–zeolites.

DR UV–vis spectroscopy has been applied to asses the Fe atoms coordination in the zeolitic framework. Fig. 2 shows UV–vis diffuse reflectance spectra of the BEA support and the different Fe BEA samples. BEA zeolite has scarcely any absorbance from ultraviolet to visible region (curve a), while Fe–zeolites exhibit strong absorbance in 200–600 nm (curves b–e), revealing the existence of various ferric ion species. The charge transfer bands for the four catalysts (BSE-1/12, BSE-1/6, BSE-1/3 and BSE-2/3) show no significant differences.

Two charge transfer bands at 250 and 350 nm are observed. The intensities of the two bands increase with the iron content. Additionally, a band around 550 nm becomes pronounced for both BSE-1/3 and BSE-2/3 catalysts, their spectra are dominated by strong and broad features at 350 and 550 nm. These changes with iron loading are in accord with the changes in the visual appearance of the calcined catalysts ranging from white/yellow (low iron loading) to brown (high iron loading). As described in the literature, the bands below 300 nm are assigned to isolated Fe^{3+} species either tetrahedrally or octahedrally coordinated [34–37]. At higher wavelengths one distinguishes bands around 280 nm for isolated octahedral Fe^{3+} complexes, around 350 nm for octahedral Fe^{3+} in oligomeric clusters and above 400 nm for bulky Fe_2O_3-like aggregates [34–38]. The present UV–vis spectra indicate that Fe–zeolites materials contain a distribution of iron species ranging from isolated ions to bulky iron oxide agglomerates. Clearly, more extensive clustering takes place with increasing Fe loading. These different Fe environments detected by DR UV–vis are closely related with the leaching of active species. Assuming that nontetrahedrally coordinated Fe species are more labile than those tetrahedrally coordinated, the high amount of Fe leached for the BSE-2/3 is a previsible result. But, when Fe species are mostly tetrahedrally coordinated into the zeolitic framework, the leaching is clearly reduced.

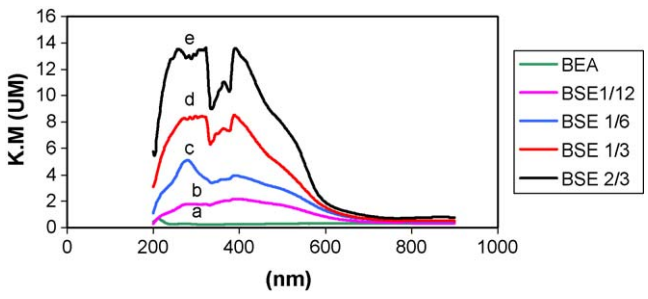

Fig. 2. UV–vis spectra of BEA matrix. BEA (a), BSE-1/12 (b), BSE-1/6 (c), BSE-1/3 (d) and BSE-2/3 (e).

Furthermore, the DR UV–vis results are in good agreement with the textural properties determined by means of N_2 analysis (Table 1). Sample with high Fe content evidences a decrease of the BET surface area and the micropore volume. The obtained data confirm the existence of Fe extra framework species that might be located within the zeolite pores correlating fairly well with DR UV–vis.

The Fe–zeolite XRD patterns looked similar, suggesting that no major loss of zeolite crystallinity has occurred (Table 1). Furthermore the Fe–zeolite X-ray diagrams did not show reflections of iron oxides. If they exist on these samples, iron oxide particles will be present in scarce amount or as very small crystallites well dispersed over the zeolite.

On the basis of the obtained results BSE-1/3 seems to be the only promising catalyst in the series in terms of catalytic activity and Fe species stability.

3.3. Catalytic activity over BSE-1/3

Once BSE-1/3 was chosen as the best catalyst, this later was retained in order to monitor the variation of pollutant concentration along 12 h reaction time of CWHO of OMW. Fig. 3 shows a similar trend of the changes of the pollutants with reaction time. As can be seen, removal of colour showed a much higher rate of increase (59%) compared to the rate of polyphenolic compounds conversion (40%) and COD reduction (30%). COD, colour and total phenols reached a nearly constant level after around 6 h of reaction time which could correspond to important depletion of H_2O_2.

Some OMW phenolic monomers were identified by HPLC. Among them, hydroxytyrosol, 3,4-dihydroxyphenylacetic acid, tyrosol and p-hydroxyphenylacetic acid were analyzed throughout the experiment using high-performance liquid chromatography. Corresponding peaks were identified by comparison of molecule retention time to standard ones.

In Fig. 4, the evolution with time of phenolic monomers concentrations is presented. From this figure it is seen that a maximum in hydroxytyrosol and p-hydroxyphenylacetic acid concentration reduction was noticed. 3,4-Dihydroxyphenylacetic acid and tyrosol were accumulated in the reaction media until 6 h time after which their concentrations start to deplete. In our previous work concerning the UV-Fenton-type oxidation of tyrosol

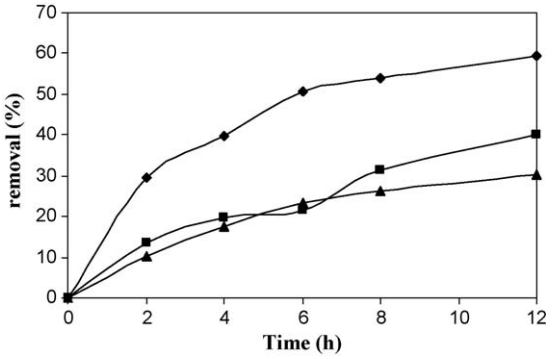

Fig. 3. CWHO of OMW over BSE-1/3 in aqueous solution as shown by evolution of COD (▲), colour (◆) and total phenol (■) with reaction time. Experimental conditions: TOC_{OMW} = 1300 mg/L, pH 5.2, T = 298 K, $[H_2O_2] = 2 \times 10^{-2}$ M, $m_{BSE\text{-}1/3}$ = 0.5 g/L.

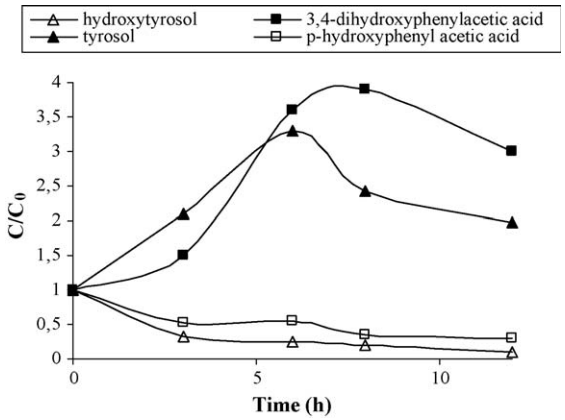

Fig. 4. CWHO of OMW in aqueous solution over BSE-1/3 in aqueous solution: evolution of phenolic intermediates concentration. Experimental conditions: TOC_{OMW} = 1300 mg/L, pH 5.2, T = 298 K, $[H_2O_2] = 2 \times 10^{-2}$ M, $m_{BSE\text{-}1/3}$ = 0.5 g/L.

[40], 3,4-dihydroxyphenylacetic acid has been identified as a reaction intermediate. So the accumulation of 3,4-dihydroxyphenylacetic acid in WHPO of OMW over BSE-1/3 catalyst can be explained by the fact that this compound is a reaction intermediate. However, the phenolic intermediates accumulation phenomenon was not observed for both model and real OMW UV-Fenton-type oxidation reaction [37]. This is probably due to the swift oxidation of intermediates. Thus interval time between intermediate occurrence and oxidation is too short to be recorded.

Treated OMW solution was tested on the *V. fischeri* bacteria by measuring the inhibition, respect to control, of bioluminescence. As shown in Table 4 a significant reduction in the microtoxicity of the wastewater could be evidenced, pointing out that the CWHO treatment is effective in reducing the toxicity and the improvement of the biodegradability, as shown by the decreasing of the COD/BOD_5 ratio of OMW after the catalytic oxidation process.

3.4. Surface reaction process

It is evident that the greater catalytic activity does not always correspond to the maximum Fe content (BSE-2/3), and it might rather be related with a better iron dispersion in the catalysts synthesized with a lower quantity of iron. According to Lin and Gurol [41], the active phase (iron) reacts with the hydrogen peroxide constituting a modified Fenton system capable of generating hydroxyl ($OH^{\bullet}$) and perhydroxil ($HO_2^{\bullet}$) radicals to carry out the oxidation of the organic molecules. The possible mechanism of OMW oxidation could be explained as follows:

$$S{-}Fe^{2+} + H_2O_2 \rightarrow S{-}Fe^{3+} + OH^- + OH^{\bullet}$$

$$S{-}Fe^{3+} + H_2O_2 \rightarrow S{-}Fe^{2+} + HO_2^{\bullet} + H^+$$

$$R{-}H + OH^{\bullet} \rightarrow R^{\bullet} + H_2O$$

where S represents the surface of the zeolite catalyst and R–H the OMW phenolic molecule.

To further understand the morphology of optimal catalyst sample (BSE-1/3) and visualize the surface reaction process, the fresh and used catalysts were characterized by electron microscopy in conjunction with EDX.

Fig. 5A illustrates the SEM image of fresh catalyst, revealing the presence of crystals of different sizes. EDX elemental analysis

Table 4
Improvement of the quality of the OMW after CWHO over BSE-1/3.

	Before CWHO	After CWHO
Toxicity (I_B%)	85	<10
COD/BOD_5	3.8	1.25

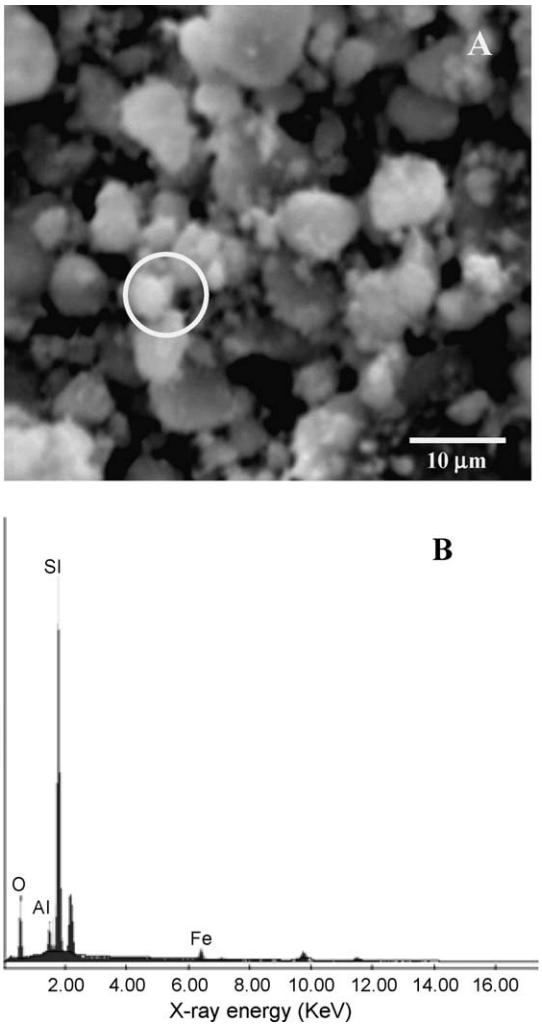

Fig. 5. (A) SEM image of the fresh BSE-1/3 catalyst and (B) EDX qualitative analysis of the selected section on (A).

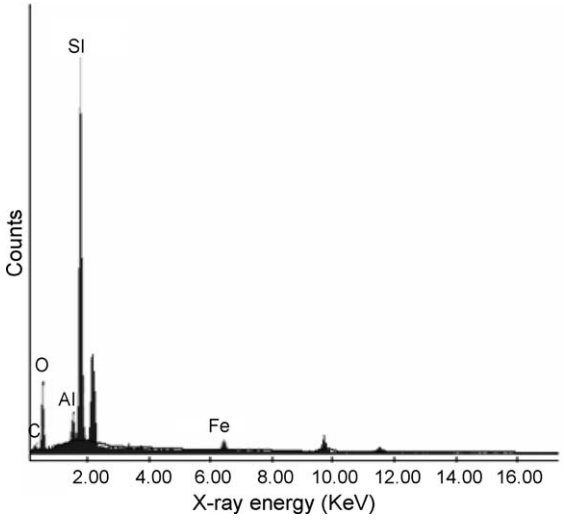

Fig. 6. The EDX qualitative analysis of the used BSE-1/3 catalyst.

Table 5
An average elemental composition of fresh and used BSE-1/3 obtained by the EDX analysis in weight%.

Samples	C	O	Fe	Al	Si
Fresh BSE-1/3	0.000	13.252	11.862	5.326	69.561
Used BSE-1/3	0.045	14.268	11.417	4.599	69.670

(Fig. 5B) over a number of selected crystals showed that they are composed of O, Al, Si and Fe.

EDX analyses of the used BSE-1/3 catalyst exhibited in Fig. 6 indicate the presence of C, O, Al, Si and Fe elements. The elemental compositions of the fresh and used BSE-1/3 catalysts found by EDX analysis in weight% are listed in Table 5. The results clearly show the appearance of C species on the used catalyst.

The addition of C element to the spent catalysts suggests the formation of congregated carbon over the iron active sites.

4. Conclusion

The present study reports on the catalytic wet hydrogen peroxide oxidation of diluted crude OMW using Fe–BEA catalysts under very mild conditions (T = 28 °C, p = 1 atm). BSE-1/3 with a moderate Fe content (Fe/Al = 1.19) is shown as a promising catalyst for the abatement of TOC (28%), OMW phenolic molecules (40%) and COD (30%). This process has evidenced an outstanding activity for the direct mineralization of OMW. Fe–zeolites UV–vis spectra indicate that Fe-catalysts contain a distribution of iron species ranging from isolated ions to bulky iron oxide agglomerates.

Catalytic wet hydrogen peroxide oxidation of OMW over BSE-1/3 matrix at very mild conditions can be considered as a suitable alternative to existing methods or applied as a pre-treatment of OMW. Dilution of OMW could be performed using urban wastewaters instead of distilled water and thus minimizing the cost of the total treatment process.

Acknowledgements

Thanks to financial support provided by the CATMED contract ICA3-CT-2002-10034.

The authors would like to thank Pr. Siglinda PERATHONER for providing us the BEA zeolite.

References

[1] V. Balice, C. Carrieri, O. Cera, Riv. Ital. Sostanze Grasse 67 (1990) 9.
[2] J. Perez, T. de la Rubia, E. Moreno, J. Martinez, Environ. Toxiol. Chem. 11 (1992) 489–495.
[3] S. Sayadi, R. Ellouz, Appl. Environ. Microbiol. 61 (1995) 1098.
[4] S.G. Velioglu, K. Curi, S.R. Camlilar, Water Res. 26 (1992) 1415.
[5] N. Gharsallah, Bioprocess Eng. 10 (1994) 29.
[6] A. Martin, R. Borja, C.J. Banks, J. Chem. Technol. Biotechnol. 60 (1994) 7.
[7] M.D. Gonzàlez, E. Moreno, J. Quevedo-Sarmiento, A. Ramos-Cormen, Chemosphere 20 (1990) 423.
[8] G. Boari, A. Brunetti, R. Passino, A. Rozzi, Agric. Wastes 10 (1984) 161.
[9] M. Hamdi, Bioresour. Technol. 36 (1991) 173.
[10] L. Plant, M. Jeff, Chem. Eng. (1994) 16.
[11] G.C. Walling, Acc. Chem. Res. 8 (1975) 125.
[12] J. De Laat, H. Gallard, Environ. Sci. Technol. 33 (1999) 2726.
[13] G. Ovejero, J.L. Sotelo, F. Martinez, L. Gordo, Water Sci. Technol. 44 (2001) 153.
[14] C. Catrinescu, C. Teodosiua, M. Macoveanu, J. Miehe-Brendlé, R. Le Dred, Water Res. 37 (2003) 1154.
[15] J.A. Melero, G. Calleja, F. Martinez, R. Molina, Catal. Commun. 7 (2006) 478.
[16] N. Crowther, F. Larachi, Appl. Catal. B: Environ. 46 (2003) 293.
[17] E.V. Parkhomchuk (Kuznetsova), M.P. Vanina, S. Preis, Catal. Commun. 9 (2008) 381.
[18] S. Caudo, G. Centi, C. Genovese, S. Perathoner, Appl. Catal. B: Environ. 144 (2007) 663.
[19] K. Fajerwerg, H. Debellefontaine, Appl. Catal. B: Environ. 10 (1996) 229.
[20] J. Barrault, M. Abdellaoui, C. Bouchoule, A. Majeste, J. Tatibouet, A. Papayannakos, Appl. Catal. B: Environ. 27 (2000) 225.
[21] E.V. Kuznetsova, E.N. Savinov, L.A. Vostrikova, V.N. Parmon, Appl. Catal. B: Environ. 51 (2004) 165.
[22] J.A. Melero, G. Calleja, F. Martinez, R. Molina, K. Lazar, Micropor. Mesopor. Mater. 74 (2004) 11.
[23] S. Valange, Z. Gabelica, M. Abdellaoui, J.M. Clacens, J. Barrault, Micropor. Mesopor. Mater. 30 (1999) 177.
[24] G. Giordano, S. Perathoner, G. Centi, S. De Rosa, T. Granato, A. Katovic, A. Siciliano, A. Tagarelli, F. Tripicchio, Catal. Today 124 (2007) 240.
[25] K. Maduna Valkaj, A. Katovic, S. Zrncevic, J. Hazard. Mater. 1441 (2007) 663.
[26] K. Fajerwerg, H. Debellefontaine, Appl. Catal. B: Environ. 10 (1996) L229.
[27] H. Kusic, N. Koprivanac, I. Selanec, Chemosphere 65 (2006) 65.
[28] S. Zrncevic, Z. Gomzi, Ind. Eng. Chem. Res. 44 (2005) 6110.
[29] G. Ovejero, J.L. Sotelo, F. Martinez, J.A. Melero, L. Gordo, Ind. Eng. Chem. Res. 40 (2001) 3921.
[30] G. Centi, S. Perathoner, T. Torre, M.G. Verduna, Catal. Today 55 (2000) 61.
[31] O.A. Anunziata, A.R. Beltramone, Z. Juric, L.B. Pierella, F.G. Requejo, Appl. Catal. A 264 (2004) 93.
[32] W.F. Hoelderich, Catal. Today 62 (2000) 115.
[33] G. Centi, G. Genovese, G. Giordano, A. Katovic, S. Perathoner, Catal. Today 91 (2004) 17.
[34] ISO 11348-2, 1998.
[35] R.J. Knechtel, J. Water Pollut. Control Fed. (May/June) (1978) 25.
[36] J.D. Box, Water. Res. 17 (1983) 511.
[37] S. Azabou, W. Najjar, A. Gargoubi, A. Ghorbel, S. Sayadi, Appl. Catal. B: Environ. 77 (2007) 166.
[38] F. Luck, Catal. Today 27 (1996) 195.
[39] F.J. Rivas, S.T. Kolaczkowski, F.J. Beltran, D.B. Mclurgh, J. Chem. Technol. Biotechnol. 73 (1998) 177.
[40] W. Najjar, S. Azabou, S. Sayadi, A. Ghorbel, Appl. Catal. B: Environ. 74 (2007) 11.
[41] S.S. Lin, M.D. Gurol, Environ. Sci. Technol. 32 (1998) 1417.